

2008

Studies of Breakdown in a Pressurized RF Cavity

M. BastaniNejad
Old Dominion University

A. A. Elmustafa
Old Dominion University

C. M. Ankenbrandt

A. Moretti

M. Popovic

See next page for additional authors

Follow this and additional works at: https://digitalcommons.odu.edu/mae_fac_pubs

 Part of the [Engineering Physics Commons](#), and the [Nuclear Commons](#)

Repository Citation

BastaniNejad, M.; Elmustafa, A. A.; Ankenbrandt, C. M.; Moretti, A.; Popovic, M.; Yonehara, K.; Kaplan, D. M.; Alsharo'a, M.; Hanlet, P. M.; Johnson, R. P.; Kuchnir, M.; Newsham, D.; Rose, D. V.; Thoma, C.; and Welch, D. R., "Studies of Breakdown in a Pressurized RF Cavity" (2008). *Mechanical & Aerospace Engineering Faculty Publications*. 49.
https://digitalcommons.odu.edu/mae_fac_pubs/49

Original Publication Citation

BastaniNejad, M., Elmustafa, A. A., Ankenbrandt, C. M., Moretti, A., Popovic, M., Yonehara, K., . . . Welch, D. R. (2008). *Studies of breakdown in a pressurized RF cavity*. Paper presented at the European Particle Accelerator Conference 2008, Magazzini del Cotone, Genoa, Italy. Conference Paper retrieved from <http://accelconf.web.cern.ch/AccelConf/e08/papers/mopp080.pdf>

Authors

M. BastaniNejad, A. A. Elmustafa, C. M. Ankenbrandt, A. Moretti, M. Popovic, K. Yonehara, D. M. Kaplan, M. Alsharo'a, P. M. Hanlet, R. P. Johnson, M. Kuchnir, D. Newsham, D. V. Rose, C. Thoma, and D. R. Welch

STUDIES OF BREAKDOWN IN A PRESSURIZED RF CAVITY*

M. BastaniNejad, A. A. Elmustafa, ODU, Norfolk, VA

C. M. Ankenbrandt, A. Moretti, M. Popovic, K. Yonehara, Fermilab, Batavia, IL

D. M. Kaplan, IIT, Chicago, IL,

M. Alsharo'a, P. M. Hanlet, R. P. Johnson, M. Kuchnir, D. Newsham, Muons Inc, Batavia, IL

D. V. Rose, C. Thoma, and D. R. Welch, Voss Scientific, LLC, Albuquerque, NM

Abstract

Microscopic images of the surfaces of metallic electrodes used in high-pressure gas-filled 805 MHz RF cavity experiments [1] have been used to investigate the mechanism of RF breakdown [2]. The images show evidence for melting and boiling in small regions of ~ 10 micron diameter on tungsten, molybdenum, and beryllium electrode surfaces. In these experiments, the dense hydrogen gas in the cavity prevents electrons or ions from being accelerated to high enough energy to participate in the breakdown process so that the only important variables are the fields and the metallic surfaces. The distributions of breakdown remnants on the electrode surfaces are compared to the maximum surface gradient E predicted by an ANSYS model of the cavity. The local surface density of spark remnants, proportional to the probability of breakdown, shows a strong exponential dependence on the maximum gradient, which is reminiscent of Fowler-Nordheim behavior of electron emission from a cold cathode. New simulation results have shown good agreement with the breakdown behaviour of the hydrogen gas in the Paschen region and have suggested improved behaviour with the addition of trace dopants such as SF_6 [3]. Present efforts are to extend the computer model to include electrode breakdown phenomena and to use scanning tunnelling microscopy to search for work function differences between the conditioned and unconditioned parts of the electrodes.

INTRODUCTION

RF cavities pressurized with hydrogen gas are being developed to produce low emittance, high intensity muon beams for muon colliders, neutrino factories, and other applications. The high-pressure gas suppresses dark currents, multipacting, and other effects that are complicating factors in the study of breakdown in usual RF cavities that operate in vacuum.

In the studies reported here, various metals were tested in a pressurized cavity where RF breakdown is expected to be due only to the interaction of the metallic surfaces with the electromagnetic fields. After exposure to the RF fields, metallic Be, Mo, Cu, and W samples were examined using a Hirox microscope and a scanning electron microscope (SEM) to measure the distribution of breakdown events on the electrode surfaces.

Apparatus

A schematic of the 805 MHz Test Cell (TC) geometry is shown in Figure 1. The TC is a cylindrical stainless

steel pressure vessel. RF power is fed into the chamber via a coaxial line. A solenoid magnet (not shown in the figure) provides an axial magnetic field of up to 3 T, which is used in some of the data sets. Replaceable hemispherical electrodes of various materials (Cu, Mo, Be, W) are separated by a 2 cm gap.

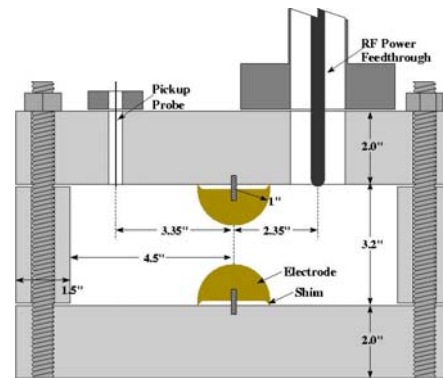


Fig. 1: Cross section of the test cell showing the replaceable one inch radius Cu, Mo, W, or Be hemispherical electrodes. The top and bottom plates and the cylinder are copper-plated stainless steel (the gas input/exhaust port is not shown in the figure).

EXPERIMENTAL RESULTS

RF breakdown

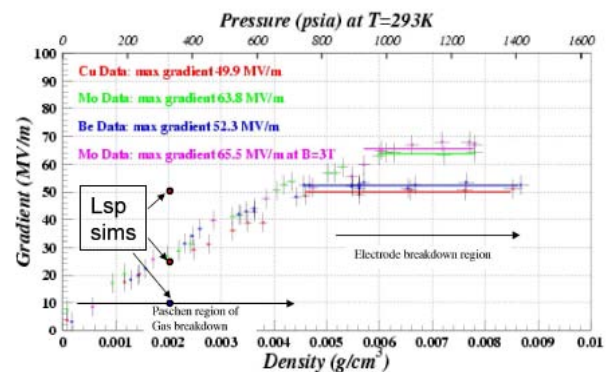


Fig. 2: Maximum stable TC gradient as a function of hydrogen gas density or pressure for Cu, Be, and Mo with no external magnetic field and Mo with 3 T. The three points labelled Lsp sims correspond to simulation results discussed below.

Increasing gas density reduces the mean free collision path for ions giving them less chance to accelerate to energies sufficient to initiate showers and avalanches. As shown in Figure 2, it is found that Cu and Be electrodes

operated stably with surface gradients near 50 MV/m, Mo near 65 MV/m, while W achieved values near 75 MV/m.

Electrode Analysis

After the exposure of the electrodes to acquire the data shown in figure 2, each electrode was examined using secondary and Hirox microscopes. The local surface density of breakdown remnants was recorded as a function of the zenith angle (zero angle corresponds to the axis of the TC). On Be, the breakdown remnants mostly look like boiled melted areas in a tadpole shape with head and tail (figure 3).

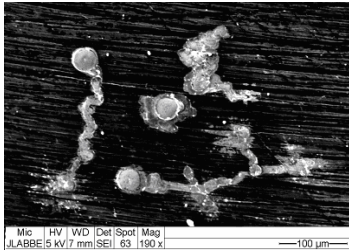
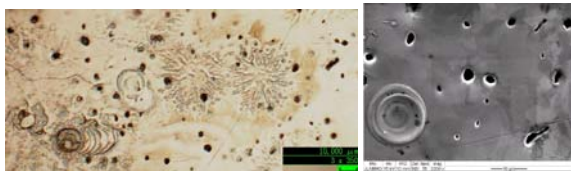


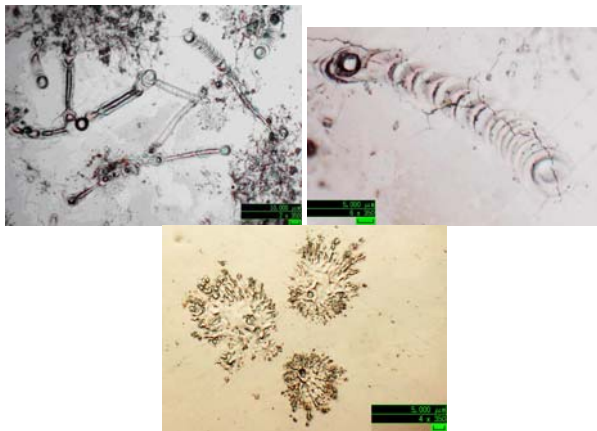
Fig. 3: Beryllium breakdown remnants.

For Mo the breakdown remnants look like overlapped circular melted regions and some splashed areas. Small holes in the melted region may be vents of metallic vapor due to boiling (Figures 4, 5).



Figs. 4, 5: Molybdenum remnants.

Tungsten breakdown remnants are furrow-shaped melted areas extended on the surface ending in a series of overlapped circles (Figures 6, 7, 8). Cracks that are seen on the breakdown areas are assumed to have occurred subsequent to breakdowns because they are seen on the last ending circle of the set of repeated circles.



Figs. 6, 7, 8: Tungsten Breakdown.

EXPERIMENTAL DATA ANALYSIS

To investigate the correlation of breakdown and the electric field, the local surface density of breakdown remnants was compared with the maximum expected electric field using an ANSYS model. Least squares fits of the data to a power of the predicted maximum electric field at the surfaces of the electrodes show good agreement for high values of the exponent. Figure 9 shows the predicted maximum surface gradient (dashed), the data (black with error bars) as described above, and the best least squares fit (red) to the data $y=0.34E^7$ versus zenith angle for Be. Figures 10 and 11 show the experimental data, the ANSYS model data, and best fits for Mo and W respectively.

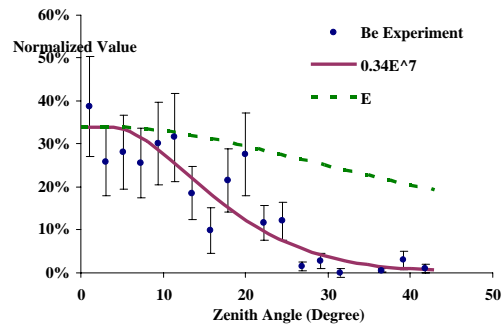


Fig. 9: Be breakdown area fraction vs. zenith angle.

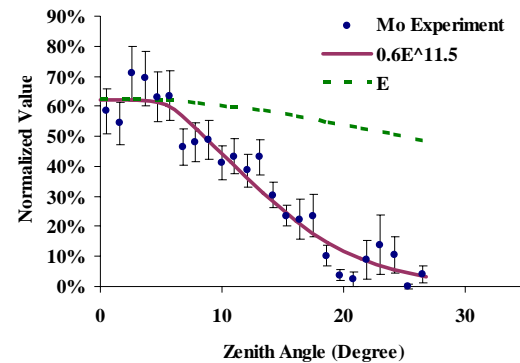


Fig. 10: Mo breakdown area fraction vs. zenith angle.

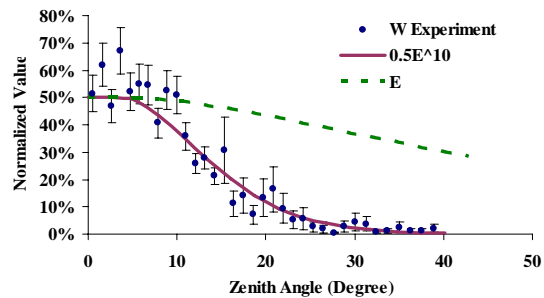


Fig. 11: W breakdown area fraction vs. zenith angle.

The plots also show that the breakdown data correlates with a high power of electric field: 7 for Be, 11.5 for Mo and 10 for W. This suggests that the breakdown is a

quantum mechanical effect described by the Fowler-Nordheim theory of field emission by tunnelling of electrons through a barrier in the presence of a high electric field.

FIRST COMPUTER SIMULATIONS

Computer calculations to simulate the behaviour of breakdown in helium-filled spark-gap switches [4] have been extended to use hydrogen in the Muons, Inc. Test Cell [5]. Three values of electric field were used for the calculations in the conditions of figure 2 at a density of $.002 \text{ g/cm}^3$ as indicated by the three red and blue dots.

Figure 12 shows the simulation results for the three electric field strengths, where the electron density is stable below the Paschen curve (10 MV/m), slightly unstable at the curve (25 MV/m), and very unstable for values above the curve (50 MV/m).

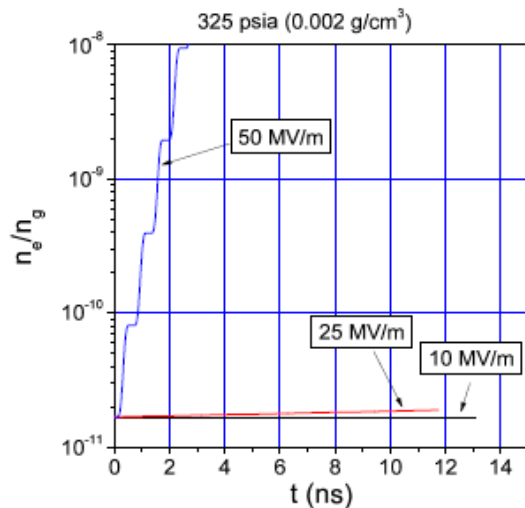


Fig. 12: Electron density as a function of time at 805 MHz and gas density 0.002 g/cm^3 .

The temporal evolution of these curves is consistent with the results of the experiment; for $E_0 = 10 \text{ MV/m}$, the electron population does not grow because the field is too low to induce ionization of the neutral H_2 . At 25 MV/m , the electron density is slowly growing, consistent with this value of E_0 being at the edge of the Paschen law breakdown limit in Figure 2. At 50 MV/m , the electric field drives electrons in the tail of the distribution to high enough energies to efficiently ionize the gas. It is interesting that the 805 MHz period is seen in the growth of the electron density.

One proposed method to increase the effective breakdown threshold for the gas at a given pressure is to introduce a low concentration of electro-negative gas to the H_2 . A very low ratio mixture of SF_6 is used to examine this effect. Three additional particle species of neutral SF_6 , SF_6^+ , and SF_6^- are added to the calculation. The results of a calculation at $E_0 = 25 \text{ MV/m}$ are shown in figure 13, which plots the electron and negative ion density as a function of time. The initial electron population rapidly decreases, as the negative ion density

increases. This demonstrates the desired effect of increasing the Paschen limit for breakdown in pure H_2 .

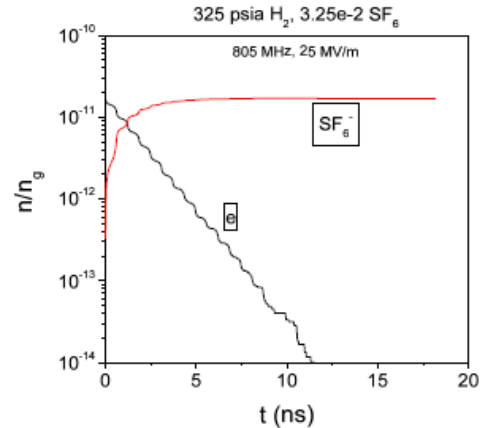


Fig. 13: Electron density depletion and SF_6 ion density growth as a function of time at H_2 density $6 \times 10^{20} \text{ cm}^{-3}$ and SF_6 density $6 \times 10^{16} \text{ cm}^{-3}$.

CONCLUSIONS

The breakdown data shown in figures 9, 10 and 11 show good agreement with high powers of electric field. This strong electric field dependence of the breakdown in pressurized gas is so similar to the dark current dependence predicted by Fowler and Nordheim that breakdown of a metal in a strong electromagnetic field is very likely also a quantum mechanical effect. The fact that the conditioned surfaces of the electrodes are rougher than the unconditioned areas implies the surface enhancement factor in the Fowler-Nordheim expression is not the dominant effect. Thus the work function is a likely factor in the ultimate breakdown limit of metallic structures. This has inspired the study of the distributions of work functions in the electrodes using scanning tunnelling microscopy. On another front, computer simulations of the Paschen region of the breakdown data of the Test Cell show good agreement. The next steps to extend the model to include the metallic electrodes may give more insight to the mechanism of RF breakdown.

REFERENCES

- [1] P. Hanlet, M. Alsharo'a, R. E. Hartle, R. P. Johnson, M. Kuchnir, K. Paul, C. M. Ankenbrandt, A. Moretti, M. Popovic, D. M. Kaplan, et al., in Proceedings of EPAC06, Edinburgh, Scotland (2006), p. 1364.
- [2] M. BastaniNejad et al., in Proceedings of PAC07, Albuquerque, New Mexico (2007), p. 2499.
- [3] Lsp is a software product developed by ATK Mission Research, Albuquerque, NM 87110.
- [4] C. Thoma, et al. IEEE Trans. Plasma Sci. 34, 910 (2006)].
- [5] D. V. Rose, C. Thoma, D. R. Welch, and R. E. Clark, Low Emittance Muon Collider Workshop, Fermilab, 2008, http://www.muonsinc.com/lemc2008/presentations/ROSE_LEMC2008.ppt